Grant Number: **NAG5-8653**

Final Equipment/Property/Material Report

You may use this as a guide regarding what information you need to submit as your Final Property Report for any grant or cooperative agreement.

Note:
Check one under Federally-owned and check one under Grantee-acquired.

I. **Federally-owned**: Federally-owned items provided to the Grantee.

    _X_ 1. There are no Federally-owned items under the subject grant.

    ___ 2. There are Federally-owned items under the subject grant.
       Disposition request and inventory are attached to this e-mail

    ___ 3. There were Federally-owned items under the subject grant which were returned to the Government on _____ (date). **Attach documentation regarding receipt by the Government.**

II. **Grantee-acquired**: Grantee bought the items with Grant funds.

    ___ 1. There are no Grantee-acquired items under the subject grant.

    ___ 2. There are no Grantee-acquired items, title to which vests with vests with Grantee, which are required to be submitted in a final inventory.

    _X_ 3. There are Grantee-acquired items, title to which vests with Grantee, which are required to be submitted in a final inventory. **The final inventory is attached to this mail.**

    ___ 4. There are Grantee-acquired items, title to which vests with the Government, which are required to be submitted in a final inventory. **The final inventory is attached to this e-mail.**

    ___ 5. As a participant in the Federal Demonstration Partnership, title vests with the Grantee to all Grantee-acquired items and the Grantee is not required to submit a final inventory.

Signature: _Tawler P O'Slau_   Date: _11/14/03_

DEPT 1	Building	Room	Name	Model	PEID	Serial Number	Acquired Date	Acquired Value
=====	=======	====	=============================	=====	=============	======	==========	========
27114	L-004		DUAL PROCESSOR, CLELRON 433	433	000000019601	5458	09/06/2000	948.00
27114	L-004		DUAL PROCESSOR, CELERON 433	433	000000019602	5448	09/06/2000	948.00
27114	L-004		DUAL PROCESSOR CLELRON 433	433	000000019603	5461	09/06/2000	948.00
27114	L-004		DUAL PROCESSOR CELERON 433	433	000000019604	5459	09/06/2000	948.00
27114	L-004		DUAL PROCESSOR CELERON 433	433	000000019605	5447	09/06/2000	948.00
27114	L-004		DUAL PROCESSOR CELERON 433	433	000000019606	5462	09/06/2000	948.00
27114	L-004		DUAL PROCESSOR CELERON 433	433	000000019607	5463	09/06/2000	948.00
27114	L-004		DUAL PROCESSOR CELERON 433	433	000000019608	5460	09/06/2000	948.00
27114	00012		INTEGRATING SPHERE, 10"CUSTOM		000000020931		08/27/2001	4,446.52

TOTAL   9f   12,030.52

REPORT OF INVENTIONS AND SUBCONTRACTS

(Pursuant to "Patent Rights" Contract Clause) (See Instructions on back)

The public reporting burden for this collection of information is estimated to average 1 hour per response, including the time for reviewing instructions, searching existing data sources, gathering and maintaining the data needed, and completing and reviewing the collection of information. Send comments regarding this burden estimate or any other aspect of this collection of information, including suggestions for reducing the burden, to Department of Defense, Washington Headquarters Services, Directorate for Information Operations and Reports (9000-0095), 1215 Jefferson Davis Highway, Suite 1204, Arlington, VA 22202-4302. Respondents should be aware that notwithstanding any other provision of law, no person shall be subject to any penalty for failing to comply with a collection of information if it does not display a currently valid OMB control number.
PLEASE DO NOT RETURN YOUR COMPLETED FORM TO THIS ADDRESS. RETURN COMPLETED FORM TO THE CONTRACTING OFFICER.

1.a. NAME OF CONTRACTOR/SUBCONTRACTOR	c. CONTRACT NUMBER	2.a. NAME OF GOVERNMENT PRIME CONTRACTOR	c. CONTRACT NUMBER	3. TYPE OF REPORT
Norfolk State University	NAG5-8653	Norfolk State University		a. INTERIM / b. FINAL [X]
b. ADDRESS	d. AWARD DATE	b. ADDRESS	d. AWARD DATE	4. REPORTING PERIOD
700 Park Avenue Norfolk VA 23504	8/31/99			a. FROM 1999/08/01 b. TO 2003/07/31

SECTION I - SUBJECT INVENTIONS

5. "SUBJECT INVENTIONS" REQUIRED TO BE REPORTED BY CONTRACTOR/SUBCONTRACTOR

NAME(S) OF INVENTOR(S) a.	TITLE OF INVENTION(S) b.	DISCLOSURE NUMBER, PATENT APPLICATION SERIAL NUMBER OR PATENT NUMBER c.	ELECTION TO FILE PATENT APPLICATIONS d.				CONFIRMATORY INSTRUMENT OR ASSIGNMENT FORWARDED TO CONTRACTING OFFICER e.	
			(1) UNITED STATES		(2) FOREIGN			
			(a) YES	(b) NO	(a) YES	(b) NO	(a) YES	(b) NO
N/A								

f. EMPLOYER OF INVENTOR(S) NOT EMPLOYED BY CONTRACTOR/SUBCONTRACTOR

(1) (a) NAME OF INVENTOR	(2) (a) NAME OF INVENTOR
(b) NAME OF EMPLOYER	(b) NAME OF EMPLOYER
(c) ADDRESS OF EMPLOYER	(c) ADDRESS OF EMPLOYER

g. ELECTED FOREIGN COUNTRIES IN WHICH A PATENT APPLICATION WILL BE FILED

(1) TITLE OF INVENTION	(2) FOREIGN COUNTRIES OF PATENT APPLICATION

SECTION II - SUBCONTRACTS

6. SUBCONTRACTS AWARDED BY CONTRACTOR/SUBCONTRACTOR

NAME OF SUBCONTRACTOR(S) a.	ADDRESS b.	SUBCONTRACT NUMBER(S) c.	FAR "PATENT RIGHTS" d.		DESCRIPTION OF WORK TO BE PERFORMED UNDER SUBCONTRACT(S) e.	SUBCONTRACT DATES f.	
			(1) CLAUSE NUMBER	(2) DATE		(1) AWARD	(2) ESTIMATED COMPLETION

SECTION III - CERTIFICATION

7. CERTIFICATION OF REPORT BY CONTRACTOR/SUBCONTRACTOR   SMALL BUSINESS or [ ] NONPROFIT ORGANIZATION [ ]

I certify that the reporting party has procedures for prompt identification and timely disclosure of "Subject Inventions," that such procedures have been followed and that all "Subject Inventions" have been reported.

a. NAME OF AUTHORIZED CONTRACTOR/SUBCONTRACTOR OFFICIAL	b. TITLE	c. SIGNATURE	d. DATE SIGNED
Shaw, Paula R. D.	Director, Office of Sponsored Programs	*[signature]*	11/13/03

DD FORM 882, DEC 2001   PREVIOUS EDITION IS OBSOLETE.

Report Period: 8/1999 – 7/2003

Design and Performance Tests of Ultra-Compact Calorimeters for High Energy Astrophysics.

Carlos W. Salgado
Norfolk State University

This R&D project had two goals: a) the study of general-application ultra-compact calorimetry technologies for use in High Energy Astrophysics and, b) contribute to the design of an efficient calorimeter for the ACCESS mission. The direct measurement of galactic cosmic ray fluxes is performed from space or from balloon-borne detectors. Detectors used in those studies are limited in size and, specially, in weight. Since galactic cosmic ray fluxes are very small, detectors with high geometrical acceptances and long exposures are usually required for collecting enough statistics. We have studied calorimeter techniques that could produce *large geometrical acceptance per unit of mass* (G/w) and that may be used to study galactic cosmic rays at intermediate energies ("knee" energies).

We were part of the ACCESS (Advance Cosmic Rays Experiment at the Space Station) calorimeter group. We participated in two ACCESS calorimeter meetings (at MSFC, Huntsville, AL) to discuss the design and construction of the ACCESS calorimeter. However, in 2001 the AO for ACCESS was indefinitely postponed. The ACCESS group opted to apply for a MIDEX mission, for which was not selected. Our calorimetry project concentrated then on studying techniques that may provide large acceptance detectors in future cosmic rays experiments.

The most important asset for detection of primary cosmic rays at and about the "knee" is *large acceptance*. To construct a large acceptance calorimeter (this term is used here in its most general accepted meaning of calorimeter as "a device to measure particle energies") the detector needs to be very light or very "shallow". We studied two possible technologies to built compact calorimeters: the use of lead-tungstate crystals (PWO) and the use of sampling calorimetry using scintillating fibers embedded in a matrix of powder tungsten. For a "very light" detector, we considered the possibility of using Optical Transition Radiation (OTR) to measure the energy (and perhaps also direction and identity) of VHE cosmic rays.

1

1. - Lead-tungstate crystals.

Our first calorimeter test was done on a borrowed PWO (lead-tungstate) crystal calorimeter prototype from the University of Giessen in Germany. After the experience obtained studying this calorimeter, we built our own prototype made from Russian and Chinese PWO crystals. We tested both using JLab photon beams.

Our first test (using the Giessen calorimeter) was done in *November, 1999*. We tested a 5x5 matrix of 2x2x20 cm^3 PWO crystals. The crystals, of Russian origin were cooled up to 8°C and kept at constant temperature of about +-0.1°C. We used a Photon tagged beam at Jefferson Lab-Hall B from an electron beam of 4.5 GeV. The photon beam was collimated to a 2mm size. Photon energies cover from 25 to 95% of the electron beam energy. We were unable to obtain the expected energy resolutions (of about 1% at 5 GeV) because of electronic noise pick up by our signal splitter and because of electron splashes produced by our collimator. We obtained energy resolutions of about 6-7%/ E. We learned several important practical lessons of how to handle the PWO crystals and how to perform precise energy resolutions in the Jlab-Hall B environment.

Our second test beam was performed *July, 2000*. We built another prototype with a totally different read-out design to overcome the electronic noise of the previous test run. We used Chinese (2x2x18 cm3) and Russian (2x2x18 cm3) PWO crystals belonging to our collaborators at Hampton University (the PRIMEX collaboration [1]). The main purpose of this test was to determine the energy and position resolution of these two kinds of crystals and compare their performances. The data was cleaner and noise-free this time. The PI presented the test results at the International Conference on Calorimetry in High Energy Physics, in October 2000 in Annecy [2], France. An energy resolution comparison between the Chinese and Russian crystals is shown in figure 1. We did not find any energy resolution measurable differences between the Russian and Chinese. However, we found problems of cross-talk and PMT's non-linearity in our assembly design. Improvements were designed and implemented.

Our next and last test of an improved PWO calorimeter (constructed by our Russian colleagues in the PRIMEX collaboration) was held in August 2001. This last test was done with several members the PRIMEX collaboration (of which the PI is also a member), as a final check on the properties Chinese and Russian crystals. Dr. A. Gasparian, PRIMEX spoke-person showed preliminary results of these studies in the International Conference on Calorimetry in High Energy Physics, in September 2002 in Los Angeles [3]. For this test a 6x6 matrix of crystals was assembled inside aluminum box (2.05x2.05x18 cm^3 single crystals). the temperature was maintained at 5 °C. Hamamatsu R4125HA were used in the read out. We measured energy and position resolutions for an incoming electron beam of approx. 4 GeV energy (defined by a pair spectrometer from e+e- pairs produced from a photon beam).. The energy resolution was measured up to 1.3 % when using a 6x6 crystal matrix, as shown in figure 2. Position resolutions depended on where the electron beam hits the crystal. The best resolutions were obtained at the edge of the crystals and were of about 1.28 mm, as shown in figure 3.
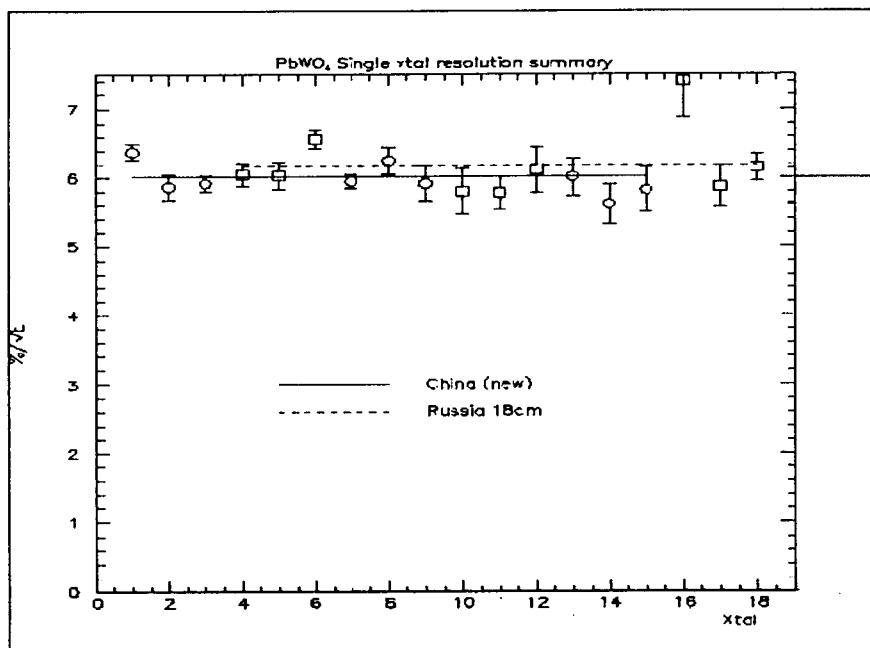
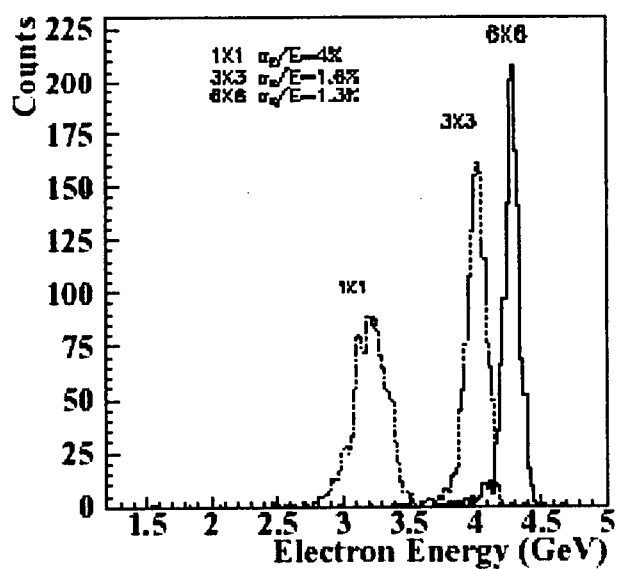**Figure 1:** Comparison between Russian and Chinese crystal's resolutions.
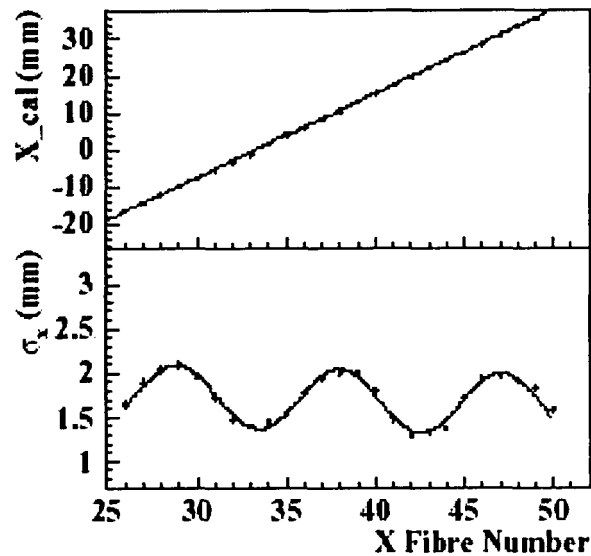

Figure 2: Energy resolution for PWO crystals.

Figure 3: Position resolutions for a PWO array as function of beam position.

2.- Sampling Tungsten Powder/SciFi.

2.1 Basic Principles

In "sampling" calorimeters the function of energy degradation (absorber material) and energy measurement (sensitive material) are separated. It has been the preferred technique in High Energy Physics for the construction of compact devices, providing a greater freedom for optimization. However, since the device measures only part of the energy, "sampling fluctuations" give rise to smaller energy resolutions. There are also several technical problems related to the use of high Z absorbers. Normally (apart from lead alloys and mixtures), these materials are difficult to machine. The optical coupling between the sensitive material (i.e., scintillating fibers) and the absorber degrades for this reason.

From table 1, we see that Uranium and Tungsten are the two pure materials with the shortest radiation length (X_0) in centimeters. Uranium is radioactive which makes it difficult to handle and creates severe constraints and limitations for on-site processing. The extreme hardness and brittleness of Tungsten has made it impossible to machine with profiles matching fibers with diameters below 1 mm. Gaps between flat plates and fibers increase the effective radiation length of the calorimeter. As a result, the sampling ratios have been limited. The use of tungsten alloys instead of pure tungsten has been considered, but a decrease of the density is obtained when even small additions of lighter materials are used. The standard material used in sampling calorimeters is lead (Pb) that, as seen from table 1, has a 60% larger radiation length (in cm) than tungsten.

4

We developed a novel idea where the absorber is made of "powder" tightly and uniformly surrounding the fibers. We used "loose" or "compressed" powder around the fibers. This technique provides almost any sampling ratio to meet the energy resolution requirements without gaps between absorber and fibers. It provides high efficiency, compactness and a variety of possibilities for having multi-channel light collection and read-out systems (important for meeting the space/mass requirements). We have been using claded plastic scintillator fibers (Bicron BCF-12) with diameters of 0.25, 0.5, 0.75 and 1,0 mm coupled to Hamamatsu PMT's readouts.

One of our most important findings has been the realization of the advantages provided by the use of *cold isostatic pressing* to carry out the compressing process. A cold isostatic press, see in figure 4, produces an uniform isostatic (Pascal type) pressure around the object to be compressed. The object is immersed in a liquid where the pressure is transmitted uniformly in all directions. This allows an homogeneous sintering of the powder *in cold* around the fibers. We have been using pressures up to 150,000 psi. Remarkable, scintillating fibers will resist (plastically) these high isostatic pressures. We are currently making precise measures on how the optical properties of the fibers are affected by isostatic pressure (if any!).

Material	Z	A	X_0 (cm)	X_0 (g/cm^2)	λ (cm)	λ (g/cm^2)	ρ (g/cm^3)
Be	4	9.0	35.3	65.3	40.6	75.11	1.85
C	6	12.0	18.8	42.68	38.0	86.26	2.27
W	74	183.8	0.35	6.75	9.58	184.9	19.3
Pb	82	207.2	0.56	6.36	17.1	194.1	11.35
U	92	238.0	~0.32	6.06	10.5	199	~18.95
BGO			1.12	7.95	22.	156.2	7.1
Lead-glass			2.54	10.36	~23.	93.8	4.08
PbF$_2$			0.93	7.22			7.77
PbWO$_4$			0.89	7.37			8.28
Shashlik			1.62				4.5
CsI			1.9	8.57			4.51
pW/SciFi			~ 0.5	~ 5.54			11.8

Table 1: Properties of common materials/detectors used in calorimeters.

In collaboration with the industry, we have obtained pure tungsten (W) powder with green densities (before pressing) of about 12 g/cm^3. This density is already superior to pure lead! (the standard material use in sampling calorimeters). These densities are obtained by a careful selection of the particle sizes in the mix ("powder characterization"). Standard tungsten powder green densities are of the order of 7 gr/cm^3. Using cold isostatic pressures up to 140,000 psi we have obtained densities of about 16.5 g/cm^3 (85% the density of pure solid tungsten).

When single or few fibers are pressed *together* within the powder, a problem arises. The compressed fibers will first reduce their sizes, but when the external pressure is released, the fibers "bounce back" to their initial dimensions and work

against the tungsten powder that remains compressed to small sizes. This "bounce back" produces a high pressure and forces that rupture the compressed tungsten matrix. We are now working on several ways to solve this problem. We have been able to compress a matrix of pure tungsten around several small tubes (0.5 mm diameter) where the fibers are later introduced (figure 5).

To understand the main characteristics of the calorimeter, we have used standard parameterizations of the electromagnetic showers [4,5,6]. A full Monte Carlo Geant4 [7] simulation for the final design is also available but it is still being developed.
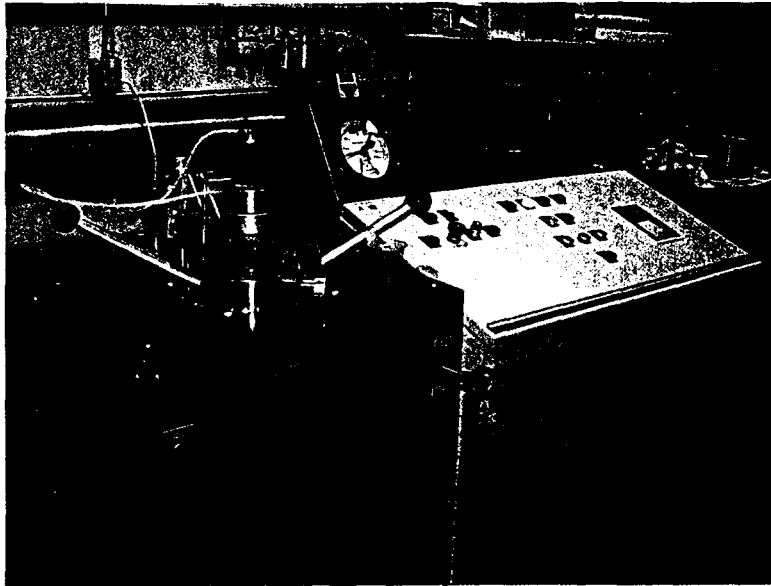
Figure 4: Cold Isostatic Press.
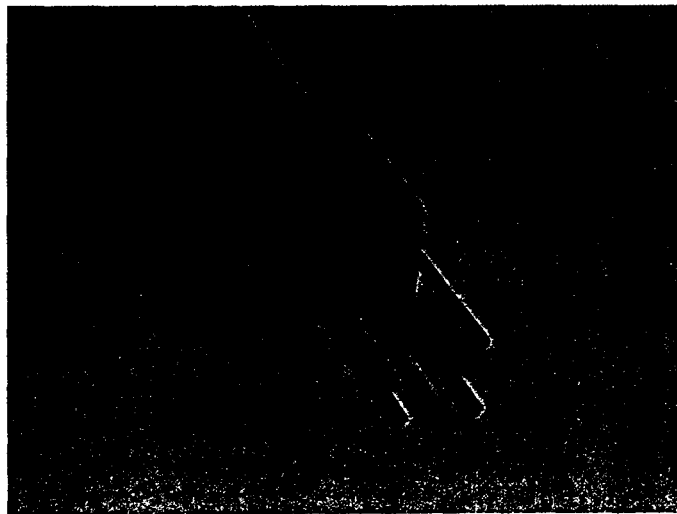
Figure 5: A prototype of a tungsten compressed matrix surrounds five steel tubing (SciFi are introduced inside).

6

For the following consideration of application, we will consider measurements of 100 GeV electrons (hadronic cosmic rays will be addressed in a future study, considering the use of the standard technique of introducing a "target " of low Z materials).

The length of a calorimeter containing 98% of the shower energy is given by:

$$L(98\%) = 2.5 \ [\ln\left(E\!\big/\varepsilon\right) + 1.2]$$

where, the length L is giving in radiation lengths, E is the incoming particle energy and ε is the critical energy given by:

$$\varepsilon = (1-y)\varepsilon_w + y\varepsilon_p \qquad\qquad \text{in MeV.}$$

For a honeycomb fiber arrangement, the plastic fraction by volume (y) is given by:

$$y = \frac{\pi}{2\sqrt{3}}\frac{\phi^2}{a}$$

where ϕ is the fiber diameter and a the distance between fiber centers. The radiation length for the mix of plastic and absorber is calculated by:

$$\frac{1}{X_0} = \frac{(1-y)}{X_w} + \frac{y}{X_p}$$

We define: $x = \rho_{POWDER}\!\big/\rho_w$ the density of powder in relation to pure W.

Therefore, the length containing 98% of the shower is given as function of x and y by:

$$L(x,y) = 2.5 \ [\ln\frac{1000}{8(1-y)x + 94y} + 1.2] \ \frac{15.05}{43(1-y)x + 0.35y}$$

and it is plotted in figure 6 versus the fiber fraction per volume (y) for three different absorber densities (x). Using compressed tungsten, we can reach a absorber density of above 80% of the pure W (about 15 g/cm^3). Therefore, using about 30% of plastic and a depth of 10 cm, most of the electromagnetic shower will be included in the calorimeter. The energy errors caused by leakage will be almost excluded.

	ρ (g/cm^3)	X_0 (cm)	ε (MeV)	$(dE/dx)_{mip}$
W Powder (loose)	11.8	0.57	8	13.5
W Powder (compress)	15.8	0.43	8	18.1
Pure W	19.3	0.35	8	22.1
Plastic	1.032	43.0	94	2.0

Table 2: Properties of material used in the Powder calorimeter.

The errors in the energy measurements will be then dominated by sampling errors. The **sampling errors** are given by:

$$\frac{\sigma}{E}\bigg|_{samp} = 0.027 \sqrt{\frac{\phi(mm)}{f_{samp}}} \frac{1}{\sqrt{E}}$$

where f_{samp}, is called the *sampling fraction*, and it is defined as

$$f_{samp} = \frac{V_{plastic}\left(\frac{dE}{dx}\right)_{mip}^{plastic}}{V_{plastic}\left(\frac{dE}{dx}\right)_{mip}^{plastic} + V_{powder}\left(\frac{dE}{dx}\right)_{mip}^{powder}}$$

therefore

$$\frac{\sigma}{E}\bigg|_{samp}(x,y) = 0.027 \sqrt{\phi(mm)\ 1+(\frac{1-y}{y})(11.05x)}$$

The sampling errors are plotted in figure 7 versus the fiber fraction per volume (x) for different fiber diameters (ϕ). With a 30% plastic fraction, one can obtain energy resolutions of the order of 1% (using 0.5-mm fibers).
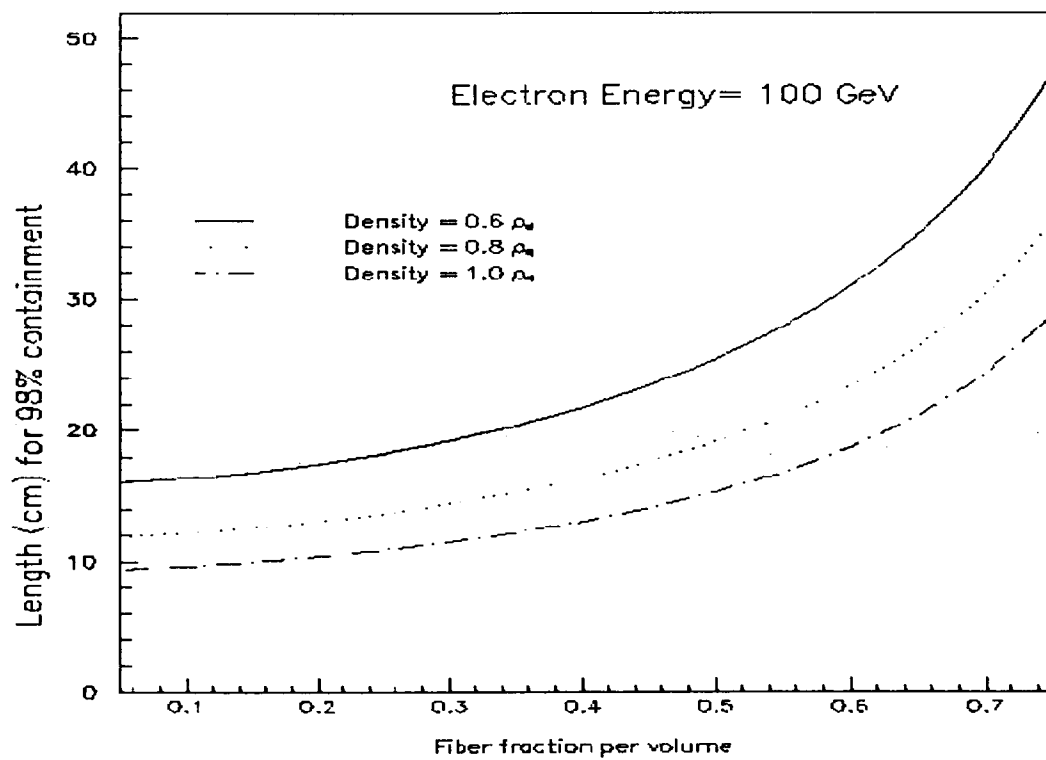
8

Figure 6: Length of 98% containment versus fiber fraction per volume in the calorimeter. The curves are for different absorber densities and all for 100 GeV incident electrons.

9

The most important advantages of this technology can be summarized as following:

♦ *The possibility of using very small (diameter) fibers.* The standard method of placing the fibers in grooves or holes is limited to 1 or 0.75 mm diameter fibers. This technology allows the use of up to 0.25-mm fibers. Therefore it is possible to reach the same energy resolution with much less fraction of plastic creating a more dense – shorter radiation length – calorimeter with the same energy resolution.

♦ We also can reach much *better resolution with less amount of plastic* per volume. For similar calorimetric conditions (resolution, leakage), the radiation length of the calorimeter is shorter. It is possible to make the calorimeter "shallower" and therefore with better geometrical acceptance.

♦ It gives *more freedom in the relative location of the fibers* inside the absorber. For example, fibers could run in layers alternating at 90° of each other, obtaining a two (or even three) dimensional measurement of the shower deposition.
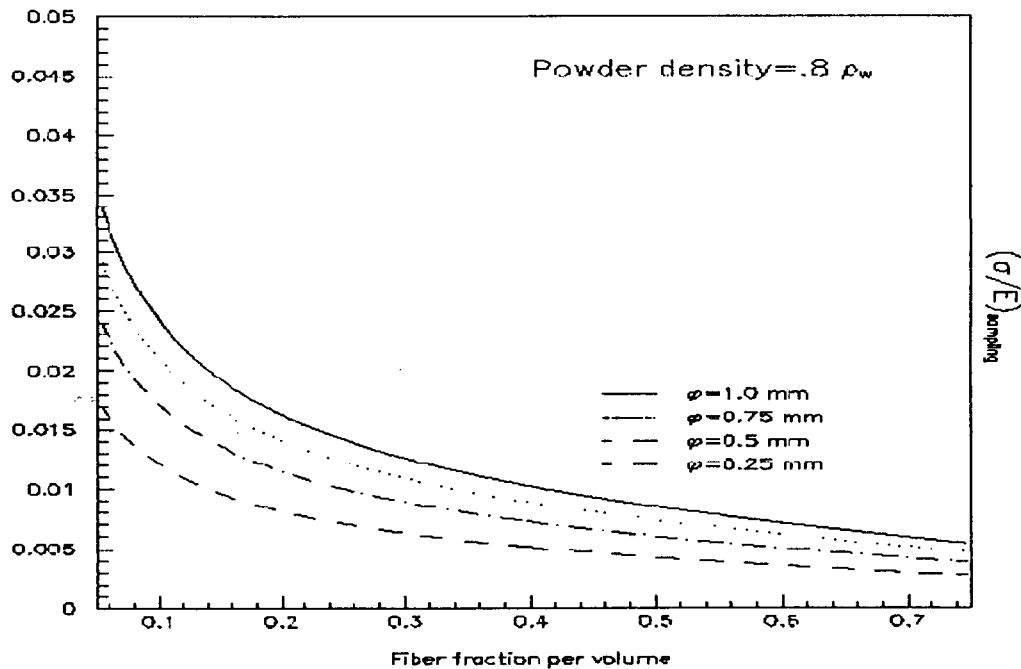

Figure 7: Relative energy resolution versus fiber fraction per volume in the calorimeter. The curves are for different fiber diameters and all for 100 GeV incident electrons.

2.2 Design, Prototypes and Tests

We have built a small prototype using "loose" powder and 0.75 mm fibers. This prototype is showed in figures 8 and 9. It is read by 24 Hamamatsu PMT's from both sides of the fibers. The characteristics of the prototype calorimeter are:

- ◆ Depth (cm): 10
- ◆ Depth (radiation lengths): 11.6
- ◆ Sampling fraction: 0.07
- ◆ 1 radiation length: 0.858 cm
- ◆ a (mm): 1.225; ϕ (mm): 0.75
- ◆ x: 0.62; y: 0.34
- ◆ Fibers/cm^2: 77
- ◆ Density: 8.14 g/cm^3
- ◆ Expected sampling error: 7%
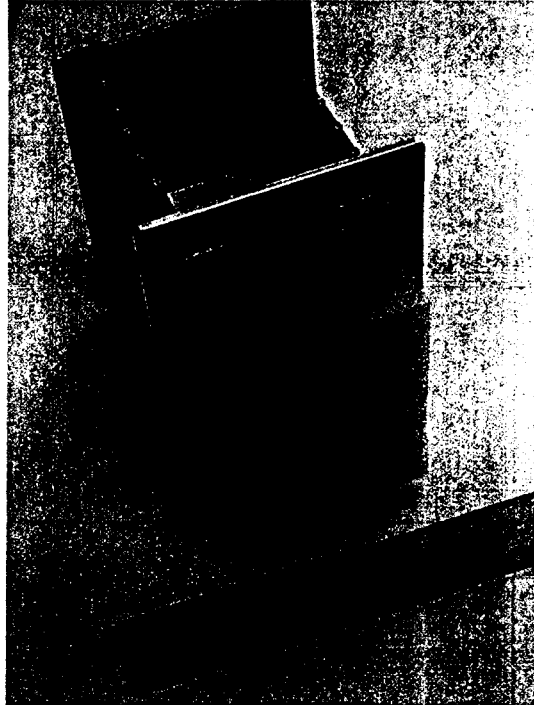
Figure 8: Small calorimeter prototype built using "loose" W powder and 0.75 mm scintillating fibers. The fibers in the front of the picture are grouped in 15 groups. Each read by a 1" PMT.

We are planning a beam test the calorimeter at Jefferson in the near future. We are currently building up the necessary electronics for the data acquisition system. We plan to design, build and continue the testing of prototypes with the purpose of studying electrons (positrons and photons) and ions (protons and heavy nuclei) in the galactic cosmic rays, when more funds will be available.
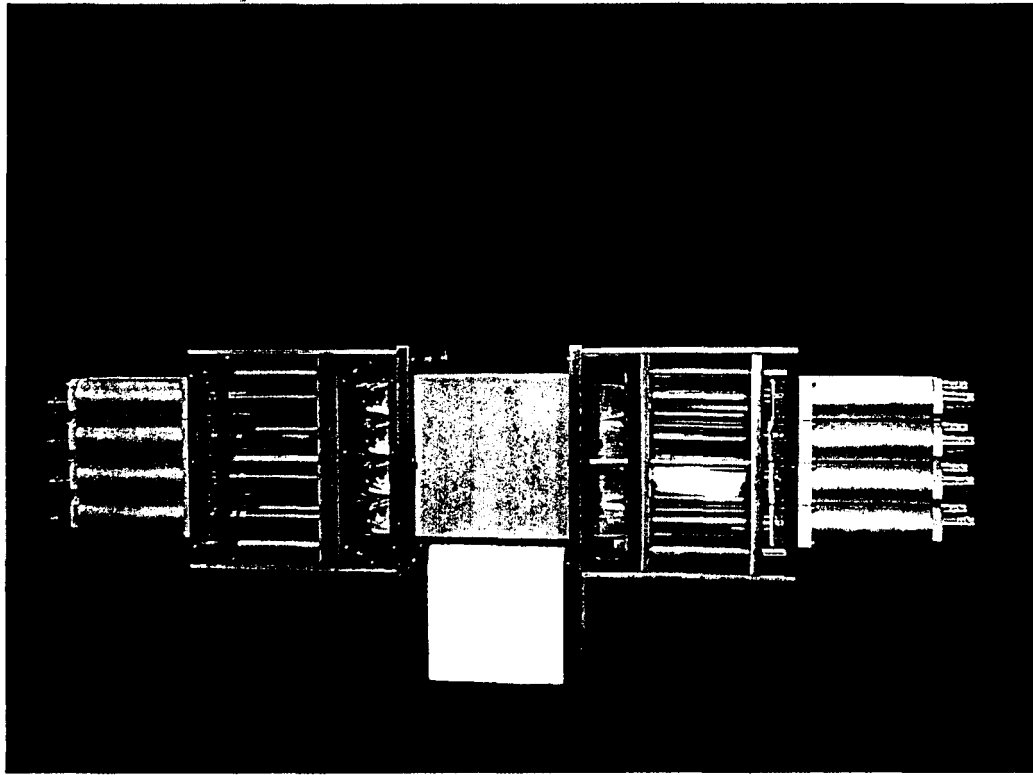
Figure 9: Powder Sci/Fi Prototype (center square) and the two sided PMT's read-outs.

Cosmic ray Calorimeter Preliminary Design

We have used a Monte Carlo method to estimate the geometrical acceptance of a trapezoidal calorimeter exposed to a uniform (in solid angle) illumination of cosmic rays. The geometrical acceptance, G (in m^2sr), is given by:

$$G = f \ \pi \ A$$

where f, is the fraction of incident particles accepted (calculated by the MC simulation) and A, is the area of the calorimeter. The following parameters has been calculated (the area A is of a square of side d):

fraction of plastic	f	depth (m)	side (m)	G (m^2sr)	mass (Ton)	total rad. lengths	G/m (m^2sr/Ton)
0.3	0.75	0.10	1.0	2.36	1.11	20	2.13

An actual experiment will have, of course, a geometrical acceptance defined by the whole detector package and not only the calorimeter. The former values are a first attempt to design a cosmic ray calorimeter based in the powder technology. The actual design will be the main objective of this proposal and will be detailed in the next section.

12

Our previous studies have been centered in the developing of the basic building techniques and not in the optimization of cosmic ray detectors. An optimization should be carried if this technique is used in an actual experiment. We have developed special tools and procedures to built the powder-W/SciFi basic modules. Each basic module (or cell) will be 1x1x10 inches^3 and contain about 200-400 scintillating fibers. We are still considering improved technologies to built the cells of compressed W powder. Those improvements will be evaluated during an initial test planned for the summer of 2003. Each cell will be read by a photo-multiplier (we are currently using R7899 1" Hamamatsu photomultipliers).

The final evaluation of the prototypes will be done optimizing a matrix that will take into account the following variables: cost, energy resolution, $\frac{\sigma}{E} = \frac{A}{\sqrt{E}} \ B$, response function asymmetries and tails, geometrical factor per unit of mass, e/h separation, e/h compensation, hadronic/electromagnetic discrimination, time resolution and angular/position resolution. We plan to write a refereed paper with the final results of these tests and simulation.

An important component in the analysis of any detector response and design is detector simulation. We will rely on the new GEANT4 code to simulate hadronic and electromagnetic showers in the detector. We had developed the expertise running the Geant4 code (it is being use to study the current small prototype). We still need to perform simulations to extrapolate our beam test results to cosmic ray energies. Unfortunately, we need to deal with energy extrapolations of several orders of magnitude and into regimes where there is too little or non-existent data for guidance.

High energy photons (electrons) are indirectly detected by the e$^+$e$^-$ pair cascades produced from their interaction with matter. The understanding of the development of the shower in a calorimeter is relatively well known, as it is based in the well-known QED theory. The relevant information about the direction of the incoming particle, background rejection and particle energy can be, then, obtained by comparison of data and simulation. For hadronic cascade simulation (i.e., incoming protons) things are more different. There is no good simulation of hadronic interactions since we do not have a well-known theory (non-perturvative QCD). There are several phenomenological based codes used to simulate hadronic interactions. The extrapolations for hadronic shower to several TeV is at best "very problematic". Electromagnetic cascade's extrapolations to higher energies are much more reliable.

Given the mass and space requirements of space or balloon-borne detectors, one critical characteristic of an actual calorimeter will be the minimum depth in radiation (nuclear absorption) lengths necessary for a good energy/angular resolution. Those values will depend on the cascade and detector characteristics. Unfortunately, cascades are by nature a random process (based in cross sections), being very difficult to discriminate between the two kinds of cascades in just a few radiation (nuclear absorption) lengths. During a few interaction lengths only a few random processes have taken place. We need to integrate over several radiation (nuclear absorption) lengths to overcome randomness. A compact calorimeter needs a "thick" absorber to rapidly develop the cascade, and a fine detector granularity to resolve the longitudinal and transverse aspects of the shower in a short space range.

13

3.- *Optical Transition Radiation (OTR).*

We tested the basic principles of transition radiation production in the visible, with the purpose of using OTR as a energy spectrometer for particles of about 1000 TeV to an expected error of about ($\delta E/E$)=50%. We had built a small prototype of several thin foils (~20μm) inside an integrating optical sphere. We took tthe prototype to CERN, during the August 2001 NASA test beam period. We tested the 1) relation between signal (number of photons) versus particle's energies, 2) the relation dependence on surface quality and 3) the relation dependence on spacing between foils. The report of this test is in appendix A.

4.- *Simulation.*

We have done simulations of isotropic illuminated volumes to find the best geometrical acceptances. We have concluded that a sphere or a cube will produce the best results. Similar results were found at the LHEA at Goddard. We have installed a 18 CPU Linux farm to help in the simulation of high energy (1000TeV) showers. We are planning to run different codes but mainly CERN's Geant4 simulation code.

We worked in a new C++ version of the simulation code (Geant4) and a parallel use of the CPU resources. We installed the Geant4 code in our Linux machines. We have tested the code in a cubic plastic calorimeter (similar to the GSFC-ACCESS design). The study of the shower backslash into the ACCESS TDR requires important low energy simulation power. The electromagnetic physics part of the simulation seems to be already in good working conditions. However, there is very little hadronic physics already activated inside the Geant4 standard code. It is our purpose to start the work on the installation and testing of the hadron interaction code onto Geant4. Specially, the hadronic interactions code is lacking the possibility of extrapolating hadronic cross sections to the VHE required for our studies.

5.- *Personnel involved in the project.*

PI: *Dr. Carlos Salgado*;
Consultant: *Dr. Youri Sharabian*, OTR and powder-tungsten/scintillating fibers design & construction of prototypes;
NSU Students: *Ilyea Shaikh* (Physics major),he worked in PWO calorimetry construction and tests. He measured the physical and optical property changes of fibers under pressure (Senior Project). *Monique Hythe* (Physics major), she worked in the design and test of cloud chambers for the detection of cosmic rays. *Tsatsu Niamadi* (Physics Major), he worked in the code for the simulation of light transmission through scintillating fibers. *Matthew Odgen* (Computer Sciences major) worked in the software for the installation of Geant4 on the NASA Linux cluster at Jlab. *Tracy Thornton* (Computer Science major), worked in coding scripts for our Linux farm and in creating a

group web page. *Jason Arcido*, measured the fiber properties under pressure in a tungsten powder matrix (Senior Project).

Other personnel involved with the project but no funded through this grant included: *Dr. Dennis Weygand* (Jefferson Lab senior scientist), and Dr. *Mina Nozar* (Research Associate Jefferson Lab/Norfolk State U.), both of them working on the Geant4 simulation and hadronic cascade physics. Dr. Nozar managed the Linux farm. *Dr. R. Srivatsan*, (NSU Research Associate) worked in the implementation of Geant4 simulation and in the construction of a cosmic ray test stand for detector calibration. *Dr. M. Khandaker* (NSU faculty member), and members of the PRIMEX collaboration (specially *Drs. A. Gasparian and D. Lawrence*) in the PWO calorimeters beam tests.

6.- Outcome

The outcomes from this proposal were technical and educational.

We have studied two possibilities for increasing the geometrical acceptance (G) per weight (w). For a trapezoidal shaped calorimeter, the geometrical acceptance approximately follows $G \approx A^2/h^2$, where A is the area and h the thickness of the detector in the vertical direction, therefore $G/w \approx A/h^3$. To increase G/w, *a "shallow" detector (short h)* is one of the possible solutions to increase this ratio. For a given energy resolution, the requirement on a large G translates to the use of materials with the shortest possible radiation length (or nuclear absorption length for hadronic calorimeters). We have studied several technical possibilities to increase the acceptance of EM, i.e., we have considered Lead-tungstate (scintillating) crystals. We favor the use of sampling calorimeters for a space or balloon-borne detectors. The advantage of PWO crystals is only in cases where good energy and position resolutions are essentials. We concluded that for studies at "knee" energies, counts are more important that resolution. PWO, and crystals in general, are more difficult to handle and much more structurally delicate than a sampling calorimeter.

The standard sampling techniques use plastic scintillators or silicon chips embedded on lead or tungsten absorbers. The absorber and sensitive materials are built on alternated layers or the sensitive materials are located on grooves or cylindrical holes machined into the absorber [3]. We have developed a new technique based in the use of compressed or loose tungsten powder as an absorber and scintillating fibers as the sensitive material.

We learned the technology of Powder Metallurgy and of how to press powder around plastic fibers without affecting the optical transmission of the fibers. Under the direction of Dr. Youri Sharabian, Jefferson Lab staff member sub-contracted under this grant, we have obtained very high "green" density powders. We obtained green powder densities of about 12 g/cm^3, compared to the standard 6 g/cm^3 green powder density. This density is already better than that of raw lead. We can increase that density up to about 18 g/cm^3 and increase mechanical strength by cold pressing.

We had reached the conclusion that the only possibility for the pressing of powder tungsten around the plastic fibers is to use a cold isostatic press. In such a press, a fluid surrounding the manufactured piece does the pressing. We obtained such

15

press (bought with JLab funds, about $75K) in October 2001. With this press, we started to compress fibers and powders to experimentally find the properties of these substances under isostatic pressure. We build several prototypes with different tungsten to plastic volume ratios. We also tested different read out possibilities.

This press is an unusual, allowing cold pressing up to 150,000 tons. Our consultant from Jefferson Lab (Dr. Sharabian) made a trip to England for training in the use of the press. We have acquired several tungsten powders with different characteristics and scintillator fibers of different dimensions. We constructed a set-up to measure the physical and optical property changes of the fibers under pressure. Two of the NSU students involved on the project (Ilyea Shaikh and Jason Arcido) wrote their senior projects on this subject.

Therefore, we developed the technique to build a viable ultra-compact calorimeter based in the new technique of compress/loose-tungsten powder that may have important technical outcomes for particle detection. Jefferson Lab is already planning the construction of a calorimeter for the upgrade of the Hall B experimental area using this technique. In places where there is not much available space or in areas of high background radiation, this technique can provide great advantages.

The scientific importance in Astrophysics and Physics of obtaining high resolution and statistics data of cosmic rays at intermediate energies is very important. It will greatly contribute to understand their origin and acceleration machanisms[9]. Several theories have recently emerged to explain the observed knee, some of which are not of astrophysical origin. Direct cosmic ray detection will be crucial to verify these arguments. The developing of new technologies to obtain larger geometrical acceptances are essential for the continue growth of cosmic ray physics.

The other important outcome of this project was educational. The involvement of minorities in the sciences is very small, and in particular, in the space sciences is almost non existent. This project brought **five** NSU students (all minorities, two of them females) in direct contact with space sciences research. Two of these students went on to graduate school, and one of them is now pursuing a graduate degree in astrophysics. Two NSU students were intensely involved in these hardware projects. Ilea Shaikh completed his senior project studying the change on optical properties of scintillating fibers under the effects of cold isostatic pressure, and Jason Arcido studied the optical transmission on fibers embedded in a matrix of compressed tungsten powder.

NSU-NPP/Jefferson Lab/NASA collaboration

Another positive outcome of this program consistent in the creation of close collaboration between Jefferson Lab, NASA and NSU. These institutions entered into an agreement in order to provide increased graduate and undergraduate opportunities for minority students in the sciences and accelerate plans for the implementation of graduate programs in sciences at NSU. This collaboration allows to expand the limited means of NSU (in laboratory space, machine shops, heavy equipment, for example) and allow fo more ambitious hardware projects, This project brought together Jefferson Lab (DOE funded National Lab) and NASA interests in solving a very similar technical problem. The result is a more efficient use of government resources that benefit equally all involved institutions.

7 References

[1] PRIMEX Experiment: - http://www.jlab.org/primex
[2] C. Salgado, Proceedings of the ICHEP, 2000.
[3] A. Gasparian, Proceedings of the ICHEP, 2002.
[4] R. Wigmans, "Calorimetry: Energy Measurement in Particle Physics", Clarendon Press-Oxford (2000).
[5] C. Fabjan, in Experimental techniques in High Energy Nuclear and Particle Physics, ed. T. Ferbel, Singapore: World Scientist. (1985).
[6] U. Amaldi, Phys. Scripta, **23**, 409, (1981).
[7] Geant 4 Collaboration, CERN - http://geant4.web.cern.ch/geant4/

APPENDIX A
Test of an Optical Transition Radiation Detector at the CERN-SPS[1]

Carlos W. Salgado and Youri G. Sharabian

Norfolk State University, Norfolk, VA 23504, USA
and
The Thomas Jefferson National Accelerator Facility,
Newport News, VA 23606, USA

Abstract

We are considering the use of Optical Transition Radiation (OTR) Detectors to measure the energy spectrum of high-energy primary cosmic rays (about and above 1000 TeV) in outer space. A very preliminary prototype of such ``calorimeter" was tested at the CERN-SPS H2 test beam-line using electrons of energies between 7 to 150 GeV. We measured light output using stacks of aluminum foils with different surface quality and distance separations.

1 Introduction

1.1 Cosmic Rays

The flux of primary cosmic rays shows an exponential drop with energies of the form $E^{-\alpha}$, where α is about 2.75. At about 5000 TeV the flux dependence on energy get still steeper, with α becoming about 3. This feature in the flux spectrum is called the "knee" and represents an important feature for the understanding of the source and acceleration of galactic cosmic rays[1].

The main problem for the experimental study of cosmic rays about knee energies is the very low flux of particles. We expect a flux of several particles per square meter per year at these energies. Due to this small flux, the study of cosmic rays around knee energies has been solely done by extensive air shower arrays (ground detectors). These experiments use the earth atmosphere as a converter and several detectors extended over a large area on the earth surface to collect the indirect signals. The properties of the primary cosmic rays are obscured by the physics of the cosmic rays interaction with atmospheric atoms[2].

Because of cost, space based detectors are severely limited on weight. To measure particle energies, detectors made of high-density materials are normally used. The standard detectors to measure high-energy elementary particles ("calorimeters") are made of very dense materials where the incoming particles are stopped and total energies are then transformed into another form of energy that can be directly measured. Detectors of this kind have been used in the past in outer space[3], but all have *low area (acceptance) per unit of weight.*

We propose to use a "light" detector to measure high-energy particle energies in space, where *the area (or acceptance) per unit of weight will be greatly improve respect to standard calorimeters.* We plan to design a detector that could be launch into orbit and provide about 25 m² of detecting area, or a detector to be able to collect a hundred events per year of primary cosmic rays with energies about and beyond the knee.

This detector will base on the Optical Transition Radiation (OTR) phenomenon.

1.2   Optical Transition Radiation

It has been known for more than 50 years that when a charged particle moves suddenly through two media of different optical properties, such particle produces electromagnetic radiation ("transition radiation")[4,5]. The emission takes place both into the forward and backward direction respect to the boundary surface. However, in the visible, due to the metal opacity only backward radiation is

detected for the incoming beam and forward for the outgoing beam through a metal foil.

In the limit of perfectly reflecting surfaces (conductors) the OTR flux angular distribution is given by[4]:

$$\frac{dW(\omega,\theta,\varphi)}{d\omega d\Omega} = \left[\frac{ze\beta \; \sin\theta}{\pi\sqrt{c}\left[1-(\beta\cos\theta)^2\right]} \right]^2 \qquad [1]$$

where θ is the angle of the emitted radiation respect to the charged particle velocity (forward OTR) or to the direction of the specular reflection of that velocity (backward OTR). ω is the frequency of the produced radiation, $d\Omega$ the solid angle of emission, φ the azimuth angle and β the particle's velocity.

Using $W(\omega, \theta, \varphi)=(h/2\pi)N(\omega, \theta, \varphi)$, where N is the number of emitted photons, and $\alpha=2\pi e^2/hc=1/137$:

$$\frac{dN(\omega,\theta,\varphi)}{\left(d\omega/\omega\right)d\Omega} = \left[\frac{z\sqrt{\alpha}\beta \; \sin\theta}{\pi\left[1-(\beta\cos\theta)^2\right]} \right]^2 \qquad [2]$$

Considering only the backward radiation (visible radiation), we integrate this equation in the frequency range where the specular properties of the surface and the light detection are the best, $[\omega_1, \omega_2]$. Also we integrate over φ in $[0, 2\pi]$:

$$dN(\theta)/d(\sin\theta d\theta) = 2z^2\left(\alpha/\pi\right)\ln\left(\omega_2/\omega_1\right)\frac{\left(\beta \; \sin\theta\right)^2}{\left[1-(\beta\cos\theta)^2\right]^2} \qquad [3]$$

For the ultra-relativistic case, $\gamma \gg 1$, this function has a maximum for:

$$\sin\theta = \left(\gamma^2-1\right)^{-\frac{1}{2}} \approx \frac{1}{\gamma} \approx \theta \qquad [4]$$

The angular distribution of OTR is peak at this value for relativistic particles. Integrating also in θ $[0, \pi/2]$, *the total number of backward OTR photons* in $[\omega_1, \omega_2]$ produced by a particle of energy $\gamma = E/mass$ is:

$$N_\gamma = z^2\left(\alpha/\pi\right)\ln\left(\omega_2/\omega_1\right)\left(\ln 4\gamma - 1\right) \qquad [5]$$

The total number of photons is logarithmically dependent on the particle energy. The energy resolution that could be achieved using the detection of OTR photons is giving by:

$$\left(\delta E/E\right) = \left(\ln 4\gamma - 1\right)\left(\delta N_\gamma / N_\gamma\right)$$ [6]

Cerenkov background

Our prototype operated at atmosphere pressure (i.e. no vacuum was used). Therefore, Cerenkov radiation was also produced by charged particles going through the air mass in the foil gaps. To estimate the Cerenkov photons we used the following semi empirical formula[6]:

$$N_\gamma = L \; N_o \; \sin^2 \theta_c$$ [7]

where, L is the length of the particle trajectory, N_o =90 cm^{-1} and θ_c is the Cerenkov angle given by: $\cos\theta_c = \dfrac{1}{\beta n}$. n is the index of refraction of the medium and β the particle's velocity.

2 Prototype

Prototypes were made of stacks of parallel aluminum foils. The OTR radiation is produced in each of the foil surfaces when electrons cross the surface (electrons come almost perpendicular to the surface in our prototype). Similar type of detectors have been used in accelerator physics[7,8,9] to measure beam profiles and at Jefferson Lab[10] to obtain beam currents. However, only one foil was used on those cases.

We tested light collection as a function of the foil's surface characteristics and the inter-foils gap distances. Four stacks with seven aluminum foils of 18-20 μm thickness each were constructed. Each foil was a circle of 0.89 inches diameter. One of the stacks is shown in figure 1 and two more stacks with different gap sizes (2 mm) and surface finishing are shown in figure 2.

The stacks were located inside a light-integrating sphere, custom made by Oriel Optics, of 10 inches diameter. A diagram of the sphere is show in figure 3, and a picture in figure 4. There are three circular holes in the sphere, two of them at 180° of each other (holes #1 and #2), and one at 90° from the others. A circular

21

buffer obstructs this last hole from viewing the beam input (and foils). The electron beam comes from hole#1 into hole #2 (see figure 3), the foil stack is attached to hole #1. A photo-multiplier (PMT) was attached to hole #3. Light will reach the PMT only after several reflections and never directly from the foils. The beam exited straight through the hole #2 (and also the Cerenkov light emitted by the electrons after the foils inside the sphere).

The inside surface of the sphere is about 99.9% reflecting, therefore mostly all light produced inside will be reaching the PMT photo-cathode through multiple reflections. We use a *Photonis* XP2262 PMT operating at a voltage of −1800V.
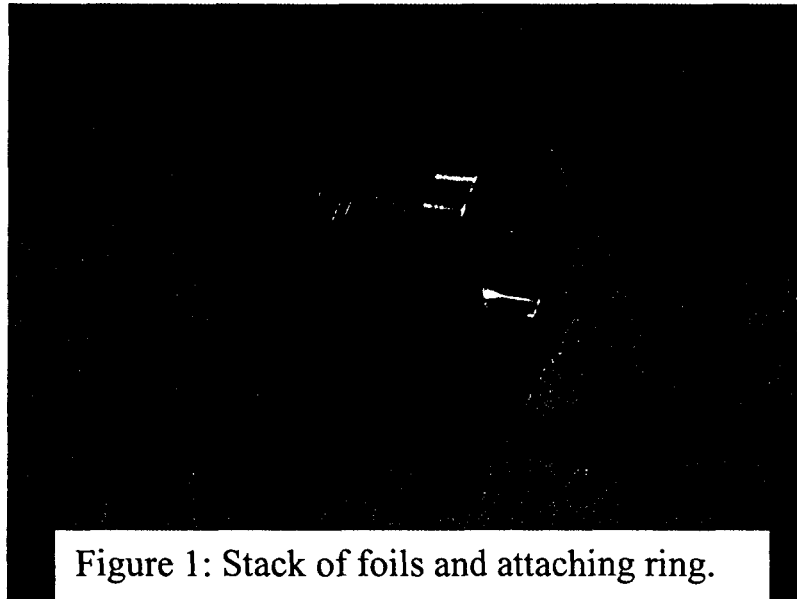
Figure 1: Stack of foils and attaching ring.

Figure 2: Foil stacks of 2 mm gap: no-polished (left) and polished (right).

#1   ELECTRON BEAM →   #2

#3
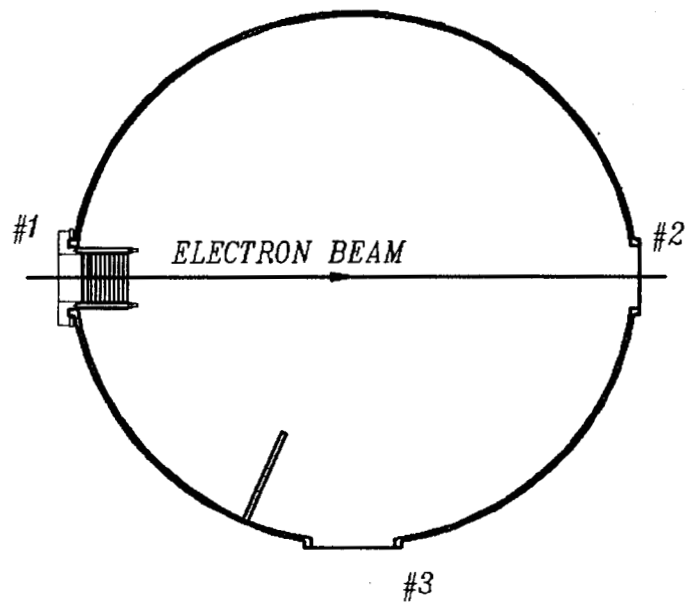
Figure 3: Diagram of the custom-made integrating sphere.
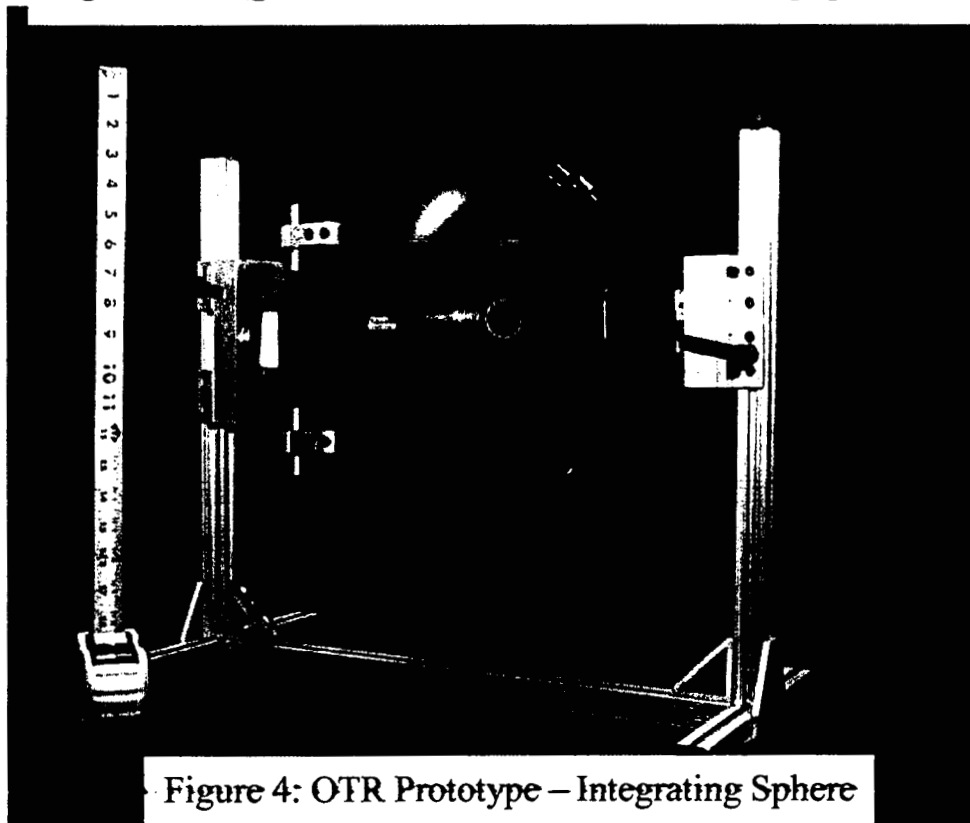
Figure 4: OTR Prototype – Integrating Sphere

3 Test

The test was done using electrons from the CERN-SPS H2 test beam line, during August 30 to September 3 of 2001. Our test was part of the "NASA-ACCESS test beam period" that included several other detector tests related to ACCESS proposals[11].

Our test was done in a "parasitic mode", since we were allowed to participate in the ACCESS test run at a late stage of the run planning. Due to these circumstances, the conditions for our test were not ideal. However, we planned for a very limited test output. Mostly, we only planned to obtain limited information regarding light collection using different gap sizes and surfaces.

Our prototype was mounted behind two TRD prototypes, from the Louisiana State University and University of Chicago groups. Those groups have priority over the running conditions. They followed a program of short (about 10-15 minutes) electron energies scan runs between 7 up to 150 GeV at low rate (between 200 Hz to 1 KHz). Taken about 100K events per run.

The electron beam structure consisted of a 5.2 sec. long spill and then a 11.6 sec. dead time, meaning a complete cycle took 16.8 sec. The amount of material in front of our prototype was changed periodically, from a minimum of 8.4 g/cm^2 to a maximum of 16.8 g/cm^2.
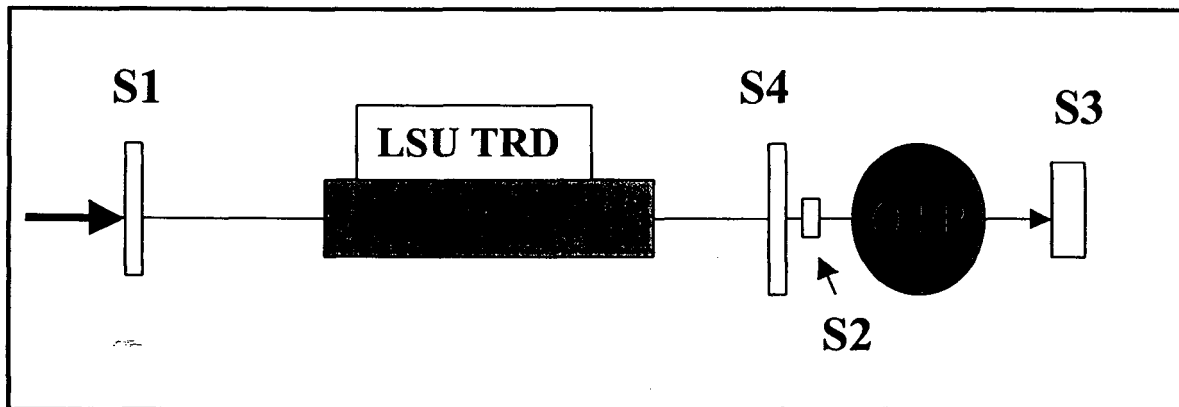

Figure 5: Test setup. The electron beam comes from the left. S1, S2, S3 and S4 are the hosdoscopes defined in the test. OTR is our prototype.

Several scintillating hodoscopes were used to define the beam and to veto on showers produced by the material on front of our prototype. The test setup is shown in figure 5. The upstream S1 hodoscope, situated at the entrance of the test area was used to define the beam into the test hall. S3 was a shower

24

counter situated just behind our prototype. It consisted of a plastic scintillator with a thin lead slab on the front to produce showers. The small S2 hodoscope was 2x2 cm^2 in size and was used to define the acceptance of our foil stacks. The LSU S4 scintillation was a larger scintillation covering the area of the sphere that can be hit by showering particles originated on the LSU TRD or upstream our setup.

Figure 6 shows a picture of the prototype setup, view from the side, behind the LSU TRD (left). The electron beam came from the left, the shower counter is shown at the right. Figure 7 shows a rear view of the setup, with the shower counter in the front of the picture. Figure 8 shows the position of the S2 and S4 hodoscopes just on front of the OTR prototype.

An ideal situation will be to have the foils on vacuum, since then no Cerenkov radiation will be present. Our prototype was not on vacuum, as we did not have enough planning time or resources to install a vacuum chamber at this time. However, Cerenkov radiation produced on the air mass inside the sphere but in the region outside the gaps was produced in the forward direction and absorbed by a darkened area (hole #2) of the integrating sphere. The Cerenkov radiation produced on the foil gaps themselves was treated as a background.
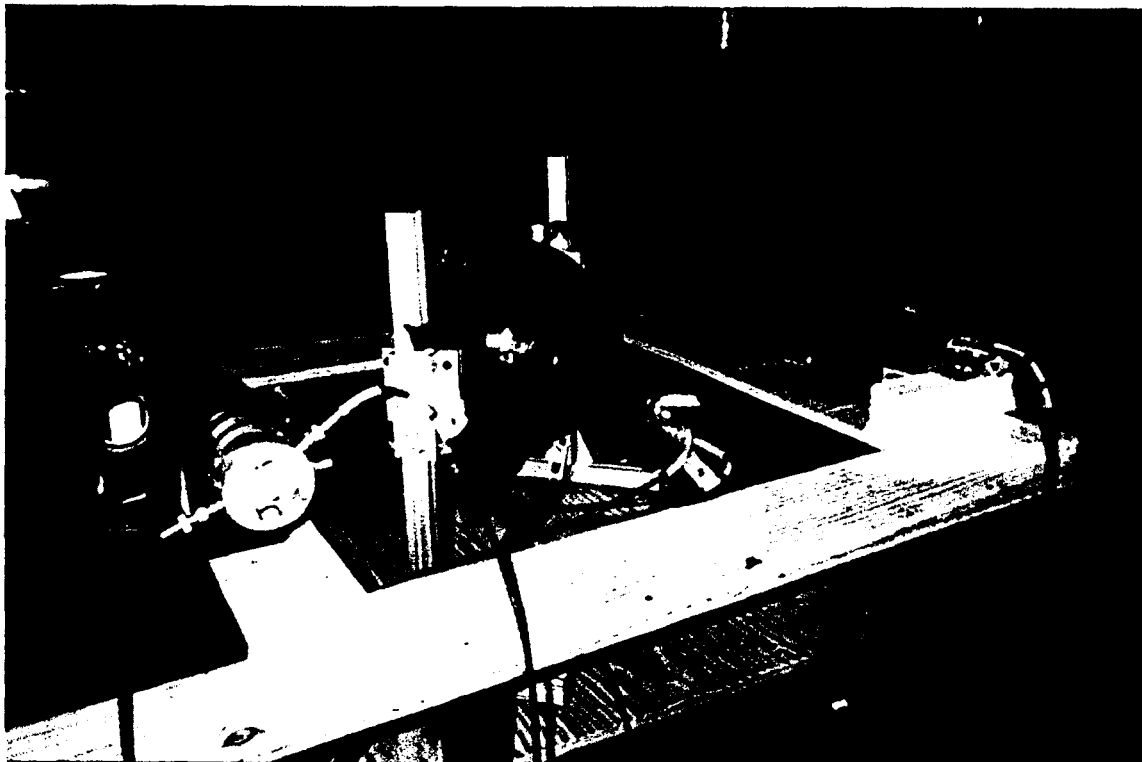

Figure 6: OTR prototype setup. Side view.

We run several configurations, listed on table 1, to obtain measurements of the light collection dependence with the gap spacing a surface quality. Most of the foil stacks were not polished. One of the 2mm stacks was polished on both sides.

#	gap (mm)	surface	LSU	beam
1	1.0	no-polished	thick -teflon	7-150 GeV
2	1.5	no-polished	thick-mylar	7-150 GeV
3	2.0	no-polished		no beam
4	2.0	no-polished	thin-teflon	7-150 GeV
5	2.0	polished	honeycomb	7-150 GeV
6	-----	no radiator	thick-teflon	7-150 GeV

Table 1: Running setup configurations.
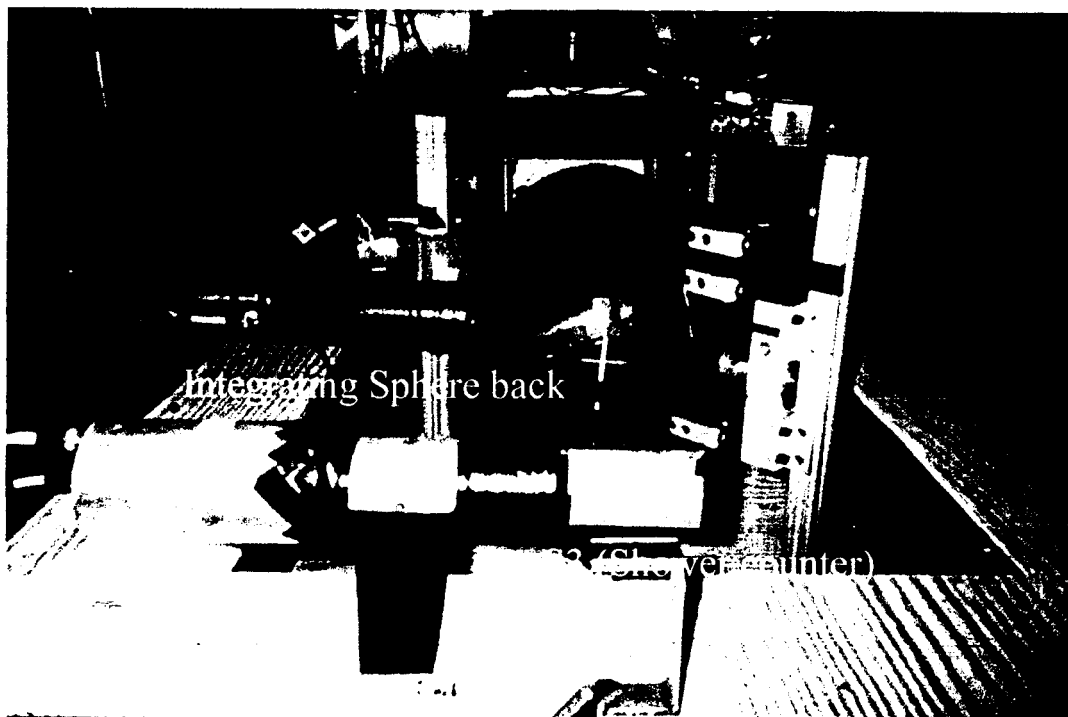
Figure 7: Prototype setup. Rear view.
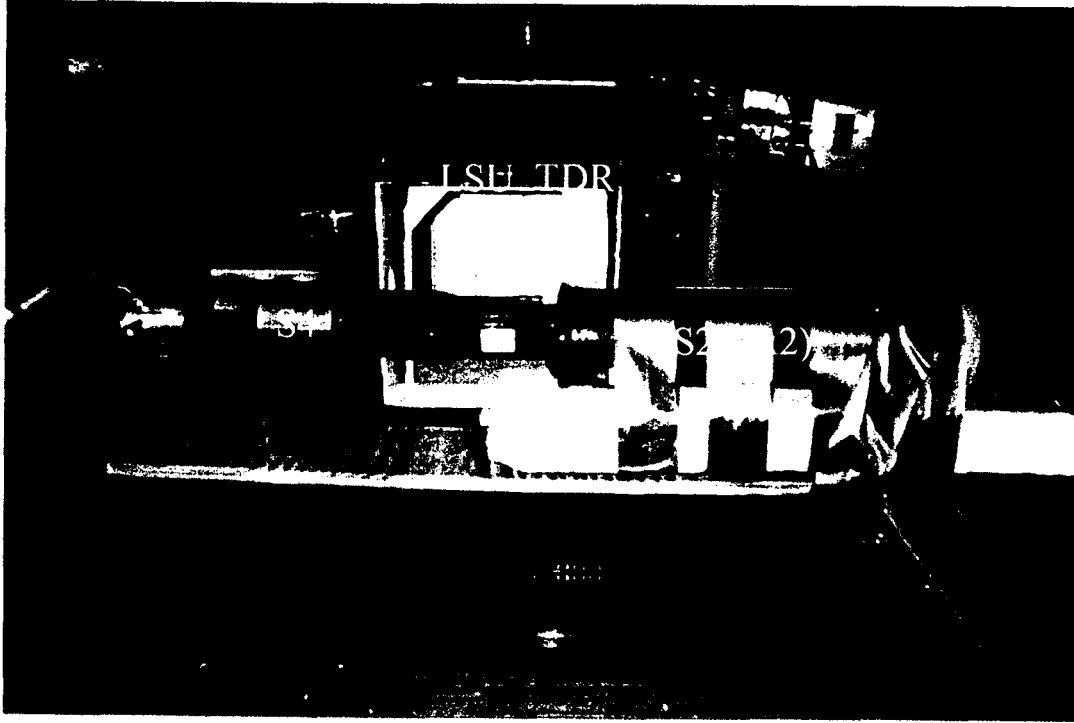
Figure 8: Prototype setup. View of the S2 and S4
hodoscopes in front of the OTR.

We used the read-out and electronics of the LSU group. Basically the DAQ took all events registered during a spill (with a signal on the S1 hodoscope) with not other trigger requirements. Our run configurations did not overlap with any unique LSU TDR configuration, therefore, conditions upstream of our prototype changed in a non-controlled way during each of our runs.

We can estimate the photon yields from OTR and Cerenkov expected by the prototype. For example, using a beam of 50 GeV electrons, we have $\gamma = 10^5$, by [5] we obtain:

$$N_\gamma \,/\, surface \ electron = \left(7.297 \ 10^{-3}/\pi\right) \, 0.6 \, \left(\ln 4 \ 10^5 - 1\right) = 0.016$$

We used 7 gaps, or 14 surfaces. Using $\varepsilon_{ph} = 0.2$ for the PMT quantum efficiency and ε_{coll} for the unknown light collection efficiency we estimated that:

$$N_{\gamma - OTR} \,/\, electron = 0.04 \, \varepsilon_{coll} \qquad [8].$$

Considering $\beta \approx 1$, we can use [7] to estimate the Cerenkov background as:

$N_{\gamma - Cerenkov} \,/\, electron = 1.4 \ 90 \ (0.02336)^2 = 0.07$. Using the same number for the quantum efficiency, we obtain $N_{\gamma - Cerenkov} \,/\, electron = 0.01 \ \varepsilon_{coll}$. We then expect at least four times more OTR than Cerenkov photons from our prototype.

27

4 Results

Data were taken at rates of 200 Hz to 1 kHz and about 100,000 events per energy setting. Due to all the material in front of our prototype, of these events only about 5-10% were kept after hosdoscope cuts. Due to the low yield of OTR production and hodoscope cuts, the data rate was not high enough to obtain the necessary statistics per energy bin. Therefore, we were not able to characterize the observed light output with the OTR logarithmic energy dependence. All our results were obtained integrating over all energies. Using [5], the expect yield variations in this energy range are of about 30%.

We took data with four OTR configurations: no polished 1mm, 1.5 mm and 2 mm and a 2 mm polished stacks. To obtain pedestal and electronic noise values, we took data with a "no-beam" configuration. Data were also taken with a "no-foils" configuration. In this last case the integrating sphere was rotate such that the beam entered from hole #1 but did not exit through hole #2. This configuration was intended for estimating the Cerenkov radiation produced by electrons on the air mass inside the sphere. It represents an upper limit to the Cerenkov background, because there was no reflection between foils involved.

Figure 9 shows the ADC spectra of the four beam hodoscopes for the four setup configurations (runs 1, 2, 4 and 5 in table 1). All runs show similar patters, although the statistics for each were different. We observe peaks corresponding to one (first peak) and multiple particles in the beam. The shower counter (S3) shows a peak produced by muons (no showering) and a wide peak produced by particles showering in the lead slab (incoming electrons). Cuts were placed, as shown in figure 9, to define *one incoming electron* simultaneously in all four hodoscopes. Between 5 to 10% of the events will survive those cuts (this percentage changed as the material in front of our prototype changed for each of the runs). Hodoscope S2 was important to define the acceptance of our foil stacks (hole #1). Hodoscope S4 was important to veto LSU-TRD originated showers that "splashed" particles into the integrating sphere but outside the foil acceptance. Those particles will otherwise create Cerenkov light backgrounds.

Figures 10 shows the OTR prototype ADC spectra for the four configurations with the beam defined by the hodoscopes. The total number of events in all plots is normalized. Superimposed to these spectra, as a shadowed distribution, figure 10 shows the ADC spectra obtained from the OTR during the no-beam run. This shadowed distribution represents electronic pedestal and noise. Each of the runs shows a clear excess of events with higher ADC counts when the beam went through the foil stacks.
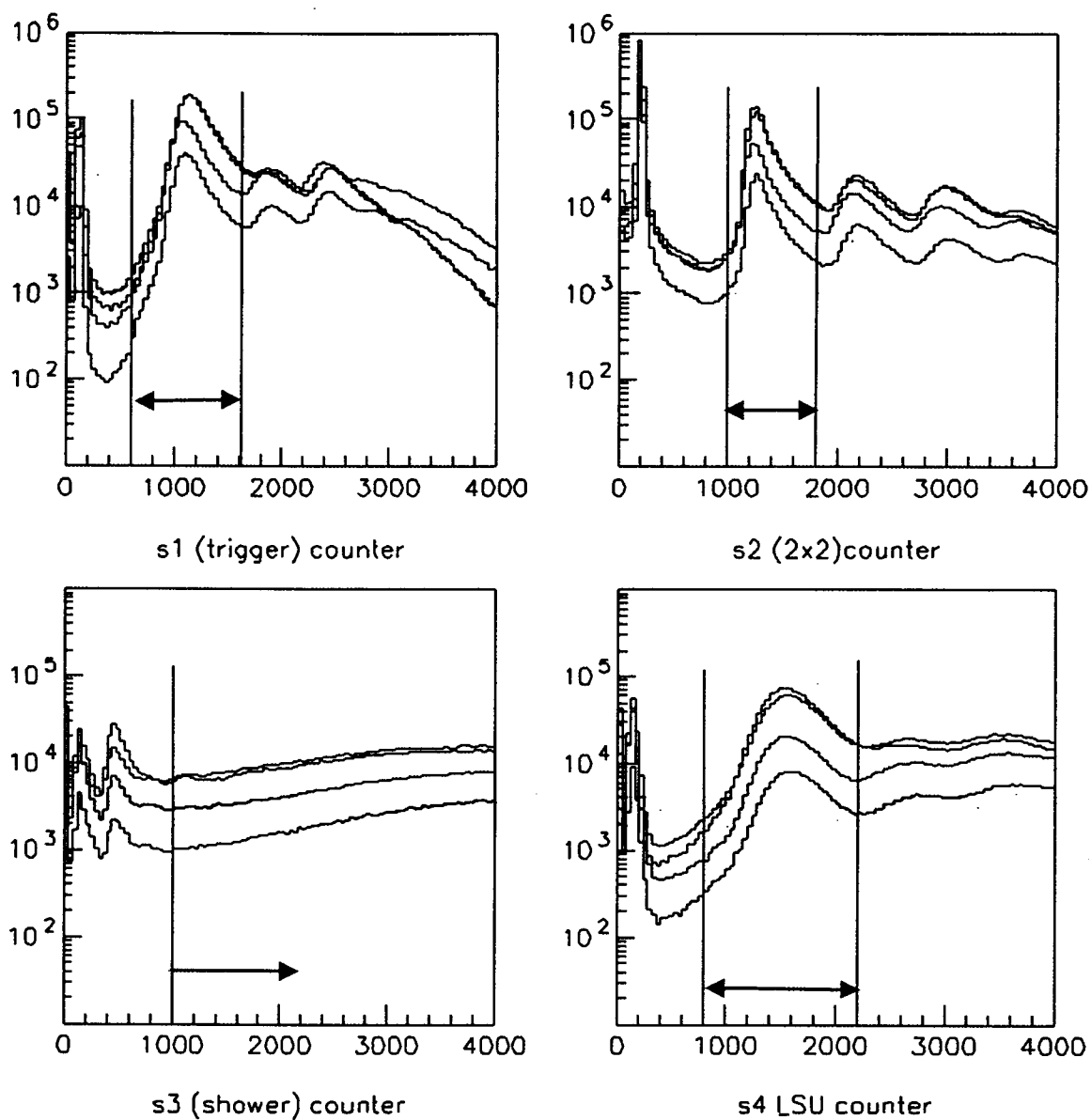
28

Figure 9: ADC spectra for the four scintillation hodoscopes.
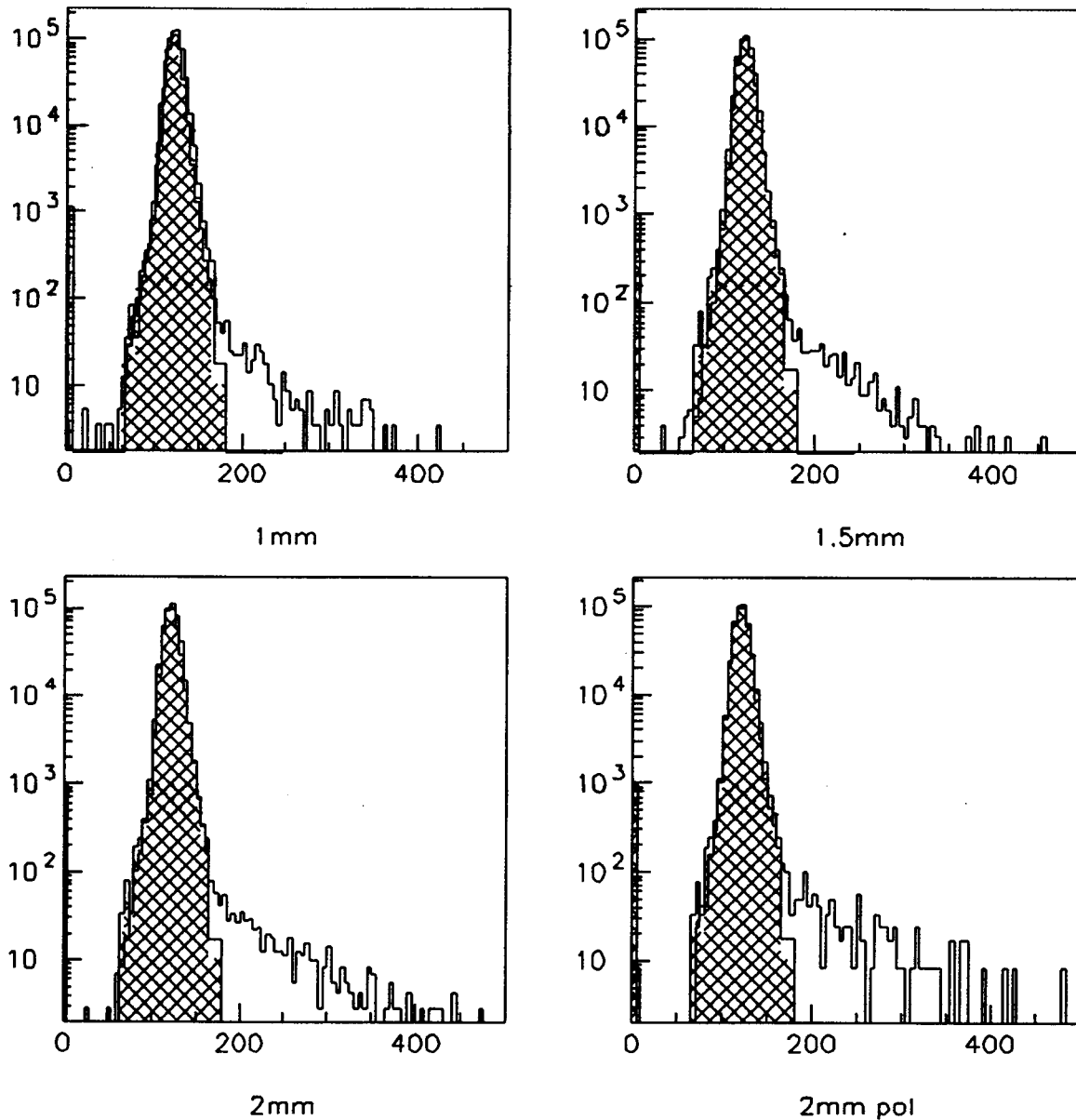Arrows mark a one charged particle (electron) cut.

29

Figure 10: OTR ADC spectra for the four configurations. The shadowed distribution was obtained for the no-beam run.

To compare light outputs among the different configuration, we count the number of events in the high end of the ADC spectra. ADC values greater than 165 were clearly produced by beam interactions with the foils. We do not have measurements on any property of the detected light (as i.e. energy or polarization dependence), therefore, we can not clearly define it as being OTR. However OTR and Cerenkov radiation are the two more feasible explanations and we expected OTR to be four times more numerous.
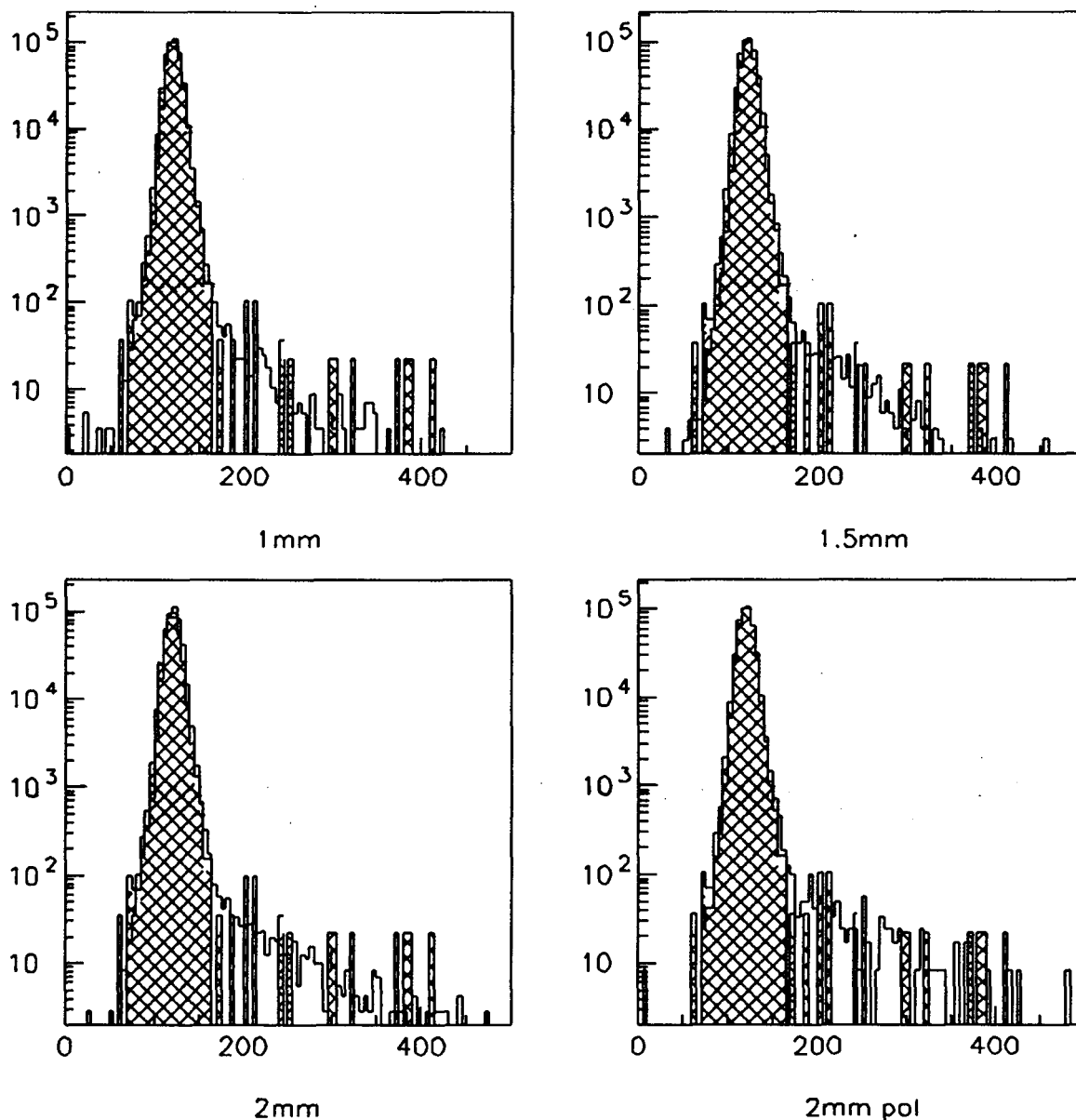
Figure 11: ADC spectra for the four OTR configuration. Superimposed in the shadowed distribution is the no-foils run ("Cerenkov bacground")

Figure 11 shows the OTR's ADC spectra for the four configurations. Superimposed are the spectra from run configuration #6 where no foils were used. The beam was passing through the full 10 inches of air mass inside the sphere. The sphere was rotated such that the sphere reflected the full Cerenkov light-cone. All Cerenkov light was trapped inside the sphere. However, as seen in figure 11, the number of ADC values greater than 165 counts is much less than the obtained with foils. Those values should give a maximum estimate for the

detected Cerenkov light. For the normal configuration, the Cerenkov light produced outside the gaps should be absorbed by the hole#2. Only the Cerenkov light produced by the air in gaps should be detected.
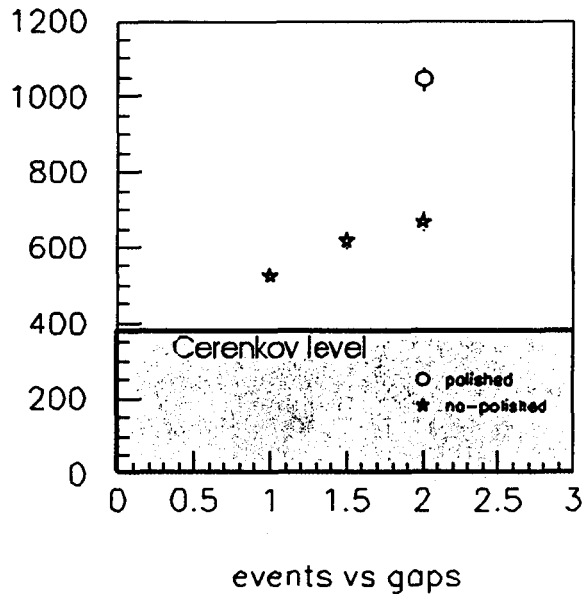

events vs gaps

Figure 12: Number of events over 165 ADC counts for the four configurations.

Figure 12 shows the integrated number of events with ADC values greater than 165 for the four foil configurations. Also show (as a level) the integrated number of events with ADC values greater than 165 counts for run #6, label as "Cerenkov level".

Our conclusions from the test can be inferred from figure 12. Increasing the gap size increases the light detection efficiency. *A polished 2 mm gap gives about 60% more light collection efficiency than the same no polished. Polished surfaces are required for reasonable efficiencies.* No polished, or "Lambertian", surfaces provide less light detection efficiencies than polished (specular) surfaces. In the case of a Lambertian surface, some light will be directed going straight to the outside of the gap for each of the reflections, however the 2mm gap since not enough to allow most of the light to come out. To the contrary, with a mirror surface, light is reflected all the way to the foil boundary to abandon the gap. Even for short gaps more light will come out in this situation.

32

Due to the changing upstream setup conditions and that our results are integrated over different beam energies is difficult to obtain an absolute value for the light collection efficiency. However, for the 2 mm polished stack, we measured that 4% of the electrons hitting the prototype produced detectable OTR light in the range defined by our ADC cut. Using [8] we obtained a value for the light collection of $\varepsilon_{coll} \approx 10\%$ in this ADC range.

5 Future Plans

We plan to continue our studies with the goal of obtaining a detector with an overall good OTR light detection efficiency (about 80%). In the future we plan to make use of 5.5 GeV electrons ($\gamma \approx 10^4$) from the Jefferson Lab accelerator. We plan to position our prototype on a vacuum chamber to eliminate Cerenkov backgrounds and to maximize light collection inside the integrating sphere. We plan to test several types of readouts and foil configurations.

Let's consider the use of an OTR detector to measure primary cosmic rays energies. We will be interested in protons with energies of about 5000 TeV, or $\gamma = 5 \cdot 10^6$ (for heavier elements things will improve because of the z^2 factor in [5]). Using [5] we have:

$$N_\gamma / surface = \left(7.297 \ 10^{-3}/\pi\right) \ 0.6 \ \left(\ln 4 \ 5 \ 10^6 - 1\right) = 0.02$$

(That is about 20% higher than this test value).
More important, using [6], the energy resolution will be:

$$\left(\delta E/E\right) = \left(\ln 20 \ 10^6 - 1\right)\left(1/\sqrt{N_\gamma}\right) = 15.8 \ \left(1/\sqrt{N_\gamma}\right)$$

Let's consider an OTR detector made of n foils. There are $2n$ surfaces and the number of expected photons per incident proton is then $N_\gamma = 0.02 \cdot 2n \cdot \varepsilon$, where $\varepsilon = \varepsilon_{ph} \cdot \varepsilon_{coll}$. Therefore:

$$\left(\delta E/E\right) = 79 \ \left(1/\sqrt{n\varepsilon}\right)$$

If we would like to obtain at least an energy resolution of $\delta E/E = 50\%$, with $\varepsilon = 0.8$, we need a detector with about n=30,000 foils. For a reasonable thickness of about 3 meters long detector, we will need a gap size of 100 μm. For light collection off such a small gap size we will need a detector composed of small pixels. If we like to build a 25 m^2 detector, of 1 μm aluminized Mylar foils, the total weight will be of around 1275 kg.

33

Due to the low yield of OTR, many crossing surfaces and good light collection are required. We believe that developing the muti-foils design or using metallic powder as OTR generating medium could finally achieve this. We plan to study the production of OTR on metallic powder. Light will be scattered (Mie scattering) through the powder cloud and then detected by high quantum efficient detectors (CCDs). This will be the topic of a future R&D project. The production of OTR light has been experimentally demonstrated. Our purpose is to obtain an efficient way to detect the produced light at the single particle level, to be able to use this phenomenon to measure particle's energies with acceptable resolutions.

6 Acknowledges

7 References

[1] V.S.Berezinskii, S.V. Bulanov, V.A. Dogiel, V.L. Ginzburg and V.S. Ptuskin, *Astrophysics of Cosmic Rays*, North-Holland, (1990).
[2] H.V. Klaptor-Kleigrothausand K. Zuber, *Particle Astrophysics*, Institute of Physics Publishing, Bristol, (2000).
[3] E.C.Stone et al., CRIS-ACE, Space Science Reviews, **86**, 283 (1998).
[4] V.L. Ginzburg and V.N. Tsitovich, *Transition radiation and Transition Scattering*, Adam Hilger, Bristol, (1990).
[5] J.D. Jackson, *Classical Electrodynamics*, John Wiley and Sons, (1975).
[6] Particle Data Book, Eur.Phys.J.,C **3**,1 (1998).
[7] P. Catravas et al.; SLAC-PUB-8190, (1999).
[8] X. Artru et al., Phys. Rev. D, **12**, 1289, (1975).
[9] C. Vernare et al., LA-UR-00-2064 (2000).
[10] V.D. Burkert et al., Jefferson Lab, CLAS-NOTE 2001-007, *An Electron Beam Monitor Based on Backward Transition Radiation*, (2001).
[11] http://lheawww.gsfc.nasa.gov/ACCESS/.